

A dynamic prognosis scheme for flexible operation of gas turbines

TSOUTSANIS, Elias <<http://orcid.org/0000-0001-8476-4726>>, MESKIN, Nader, BENAMMAR, Mohieddine and KHORASANI, Khashayar

Available from Sheffield Hallam University Research Archive (SHURA) at:

<http://shura.shu.ac.uk/16178/>

This document is the author deposited version. You are advised to consult the publisher's version if you wish to cite from it.

Published version

TSOUTSANIS, Elias, MESKIN, Nader, BENAMMAR, Mohieddine and KHORASANI, Khashayar (2016). A dynamic prognosis scheme for flexible operation of gas turbines. *Applied Energy*, 164, 686-701.

Repository use policy

Copyright © and Moral Rights for the papers on this site are retained by the individual authors and/or other copyright owners. Users may download and/or print one copy of any article(s) in SHURA to facilitate their private study or for non-commercial research. You may not engage in further distribution of the material or use it for any profit-making activities or any commercial gain.

A dynamic prognosis scheme for flexible operation of gas turbines

Elias Tsoutsanis^{a,b}, Nader Meskin^{a,*}, Mohieddine Benammar^a, Khashayar Khorasani^c

^aDepartment of Electrical Engineering, College of Engineering, Qatar University, Doha, Qatar

^bSchool of Engineering, Emirates Aviation University, Dubai, United Arab Emirates

^cDepartment of Electrical and Computer Engineering, Concordia University, Montreal, Canada

Abstract

The increase in energy demand has led to expansion of renewable energy sources and their integration into a more diverse energy mix. Consequently the operation of thermal power plants, which are spearheaded by the gas turbine technology, has been affected. Gas turbines are now required to operate more flexibly in grid supporting modes that include part load and transient operations. Therefore, condition based maintenance should encapsulate this recent shift in the gas turbine's role by taking into account dynamic operating conditions for diagnostic and prognostic purposes. In this paper, a novel scheme for performance-based prognostics of industrial gas turbines operating under dynamic conditions is proposed and developed. The concept of performance adaptation is introduced and implemented through a dynamic engine model that is developed in Matlab/Simulink environment for diagnosing and prognosing the health of gas turbine components. Our proposed scheme is tested under variable ambient conditions corresponding to dynamic operational modes of the gas turbine for estimating and predicting multiple component degradations. The diagnosis task developed is based on an adaptive method and is performed in a sliding window-based manner. A regression-based method is then implemented to locally represent the diagnostic information for subsequently forecasting the performance behavior of the engine. The accuracy of the proposed prognosis scheme is evaluated through the Probability Density Function (PDF) and the Remaining Useful Life (RUL) metrics. The results demonstrate a promising prospect of our proposed methodology for detecting and predicting accurately and efficiently the performance of gas turbine components as they degrade over time.

Keywords: Gas turbine, Prognostics, Diagnostics, Operational flexibility, Adaptive methods

Highlights

- A prognosis scheme for predicting the performance of gas turbine components is presented.
- The proposed prognosis scheme takes into consideration flexible and dynamic operating conditions of gas turbines.

*Corresponding author

Email address: nader.meskin@qu.edu.qa (Nader Meskin)

- The performance of the scheme is tested under transient conditions of gas turbines.
- The proposed scheme is utilized to detect and forecast compressor fouling and turbine erosion.

Nomenclature

Acronyms

AB	Accuracy Bounds
DI	Diagnostic Index
EoL	End of Life
ERUL	Equivalent Remaining Useful Life
GPA	Gas Path Analysis
ISA	International Standard Atmosphere
NN	Neural Networks
OF	Objective Function
PDF	Probability Density Function
RUL	Remaining Useful Life

Symbols

a	coefficient of linear regression model
l	time length of diagnostic window overlap (h)
L	time length of diagnostic window (h)
\dot{m}	mass flow rate (kg/s)
n	total number of operating points
N	corrected shaft rotational speed
p	probability
P	pressure (Pa)
q	total number of diagnostic windows
t	time instant (h)
T	temperature (K)
\mathbf{u}	ambient and operating conditions vector
W	component work (W)
x	variable
\mathbf{X}	component characteristics vector
\mathbf{Y}	measurement vector

Greek

α	accuracy bound
Γ	mass flow capacity
Δ	deviation
ϵ	average prediction error
η	isentropic efficiency
μ	mean
π	pressure ratio
σ	spread

Subscript

<i>amb</i>	ambient
<i>c</i>	compressor
<i>cl</i>	clean
<i>d</i>	diagnosis
<i>deg</i>	degraded
<i>des</i>	design point
<i>e</i>	effective
<i>f</i>	fuel
<i>inj</i>	injected
<i>lreg</i>	linear regression
<i>p</i>	prognosis
<i>pred</i>	predicted
<i>pt</i>	power turbine
<i>r</i>	reference engine
<i>ref</i>	reference
<i>t</i>	turbine
<i>th</i>	thermal
<i>thr</i>	threshold
1 – 6	engine gas path station

1 **1. Introduction**

2 The ever-growing demand for environmental friendlier and more efficient power generation sources has
3 triggered a diverse family of challenges that have to be met by gas turbines which are the prime movers

4 of thermal power plants. One of these challenges involves the **development of high fidelity, accurate and**
 5 **computationally efficient health monitoring, diagnostic and prognostic schemes for ensuring a reliable and**
 6 **effective gas turbine asset management** [1].

7 Efficiency still remains as one of the top priorities of gas turbine manufacturers and users. However, there
 8 has been a significant shift towards products that can operate with increased reliability and flexibility in load
 9 following and grid supporting roles. A significant part of this shift is due to the fact that gas turbine power
 10 plants have to compensate for intermittent renewable energy sources in a more diverse energy mix. This
 11 new type and mode of gas turbine operation has been recently implemented in the Siemens Flex-Power™
 12 [2] and GE's FlexEfficiency™ [3] technologies. A typical gas turbine operating profile is shown in Fig. 1.

13 The recent trend for increased flexibility in gas turbine operation implies that the engines are required
 14 to start up and shut down faster, and at the same time produce power at high thermal efficiency. Since the
 15 power output available from renewable energy sources is prioritized in the grid, the gas turbines will have
 16 a supporting role for fulfilling the energy demands depending on the wind capacity and the solar radiation.
 17 Consequently, majority of the gas turbine's new operating profile will be dominated by part-load operation,
 18 followed by fast start ups and shut downs as depicted in Fig. 1. This increased demand on the gas turbine
 19 flexibility has motivated the gas turbine community to evaluate the effects of this transition in terms of
 20 accuracy of diagnostic and prognostic schemes.

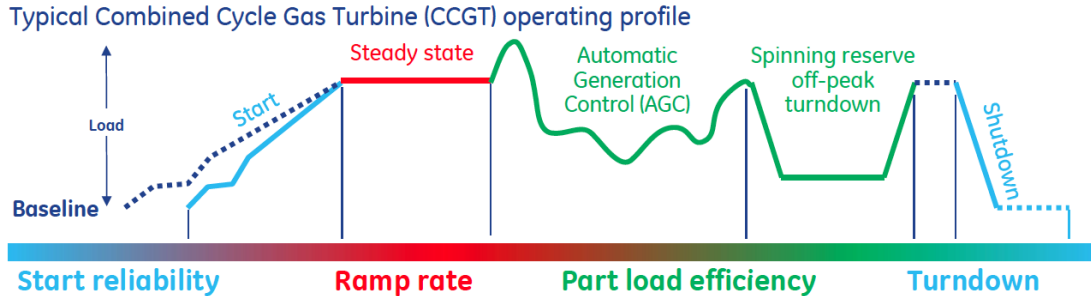


Figure 1: Flexible gas turbine operating profile [3], Courtesy of General Electric ©.

21 **Apart from a limited number of works in the literature [4, 5, 6, 7] most diagnostic and subsequently**
 22 **prognostic schemes have been developed based on the steady state performance operation.** Moreover, in
 23 dynamic operating conditions the useful life of gas turbine components is consumed faster than the steady
 24 state and the maintenance intervals suggested by manufacturers [8] are brought out forward, as shown from
 25 Fig. 2. The peaking unit given in Fig. 2 refers to a unit where its operational profile is characterized by an
 26 increased number of start ups and shut downs which characterize the transient conditions. The midrange
 27 unit refers to a unit that is dominated by part-load operations with a smaller number of start ups and shut
 28 downs, and the continuous unit refers to a unit that operates most of its lifetime at base load mode.

29 The problem of prognosis deals with prediction of the future condition of a system. The most common

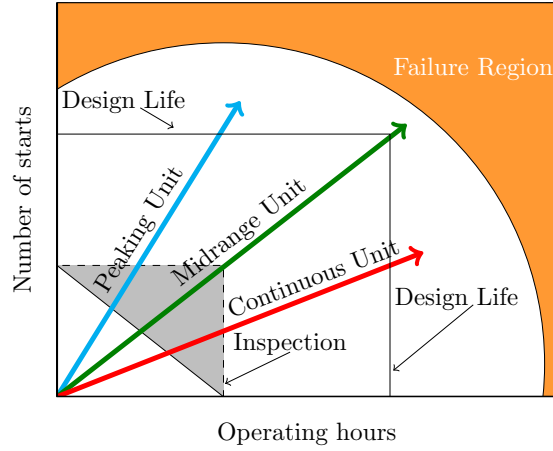


Figure 2: Gas turbine maintenance intervals for various operational modes with respect to the number of starts and operating hours as reproduced from [8], Courtesy of General Electric ©.

30 issue in prognostics deals with calculation of the Remaining Useful Life (RUL) [9, 10] of a life limited
 31 component of the system. In particular, for gas turbine prognostics there are several available methods,
 32 such as model-based [11], data-based [12, 13] and statistical [9, 14] approaches, although these schemes
 33 are only tested and developed when diagnosis is performed at steady state conditions. The capabilities
 34 of a prognosis scheme for implementing the engine’s dynamic transient performance information has to be
 35 further investigated. Among a wide selection of methods, such as exponential models [15] and particle
 36 filtering [11, 16] that are applied for prognostics of various energy systems the most common method for gas
 37 turbine prognosis is trending through regression fitting of gas turbine component degradations as developed
 38 in [9].

39 In comparison to our earlier works on transient diagnostics [17, 18], in this study the proposed adapta-
 40 tion method is further developed and implemented for gas turbine prognostics. Specifically, the proposed
 41 prognosis scheme is not continuous as suggested in [9], where all the past diagnostic results under steady
 42 state operation were used to fit a multiple regression model based on a data skewness criterion. In contrast
 43 to [9], in this study a linear regression method is implemented that is based on a local window-based seg-
 44 ment. Furthermore, the proposed scheme takes into consideration the transient operations, variable ambient
 45 conditions as well as multiple component degradations.

46 Our proposed prognosis scheme within a local window-based segment is fundamentally different from the
 47 conventional forecast of engine health and RUL based on pattern recognition methods that utilize the entire
 48 historical operating data of the engine. **The main reason for this change in the prognosis approach lies in the**
 49 **fact that most existing gas turbine prognosis schemes [1, 12, 13] rely on diagnostic methods that have been**
 50 **tested only for steady state operating conditions. In addition, for model-based diagnostic algorithms, such**
 51 **as the Gas Path Analysis (GPA), it is a common practice to take into account engine historical data that**

52 are close to the International Standard Atmosphere (ISA) conditions to minimize the uncertainty involved
53 with measurement corrections when these are corrected back to ISA conditions [9]. This type of correction
54 enables the gas turbine users to compare the health of their gas turbine assets, expressed in terms of the
55 component efficiency and mass flow rate, with the ones that are provided by the manufacturer at the ISA
56 conditions.

57 Given that the gas turbine's role is becoming more flexible, the rate of engine component degradations
58 at such dynamical operational modes will significantly change their degradation patterns and their corre-
59 sponding RUL will be shorter. Performing prognostics that take into account the entire set of operational
60 data which encapsulate the increased number of the firing start ups, shut downs and extended periods of
61 inactivity for the new type and mode of flexible operational gas turbines will produce results that will be
62 difficult to interpret for condition based maintenance. It is more practical and realistic for such types of
63 flexible gas turbine units to forecast the engine components health for a shorter time frame that will be
64 based upon the previous diagnostic results window that cover only the recent history of the engine operation.
65 Therefore, the proposed prognosis scheme may provide the gas turbine users with an improved insight on
66 the engine's health at such dynamical operating conditions.

67 Generally speaking, the accuracy of a prognosis is dependent on the diagnosis accuracy. From a series
68 of available gas turbine diagnostic methods [19] such as model-based GPA [9] and data-based [20, 21, 22]
69 approaches only a few [7, 23, 6, 24, 4, 5] have been tested for transient conditions. This study will develop
70 and implement an adaptive diagnostic method that has been successfully applied and tested for engine
71 dynamical conditions in our earlier work [17]. The advantage of this approach is that it can satisfy at a
72 high level of accuracy and low computational complexity and time a set of objectives ranging from the
73 component map reconstruction and the engine model tuning up to an effective diagnosis of degradations
74 that are experienced by multiple engine components [25].

75 An additional challenging aspect of the prognosis task is the fact that model-based gas turbine diagnostic
76 methods are heavily relying on the engine model [1]. On principle the accuracy of a gas turbine model
77 depends on detailed understanding of its components behavior as captured by component performance
78 maps. The former challenges have been effectively addressed in our earlier works [26, 18], where a number
79 of component map modeling approaches have been proposed and implemented in a dynamic engine model
80 that was developed in Matlab/Simulink, and successfully tested for the gas turbine performance adaptation.
81 It is well-known that model-based gas turbine prognostics is a challenging task since it integrates a series of
82 processes and suggested technologies [27].

83 Our proposed method is applied to a model of a two-shaft gas turbine that is injected with soft multiple
84 component degradations over time to illustrate and demonstrate the effectiveness of our approach. The
85 capabilities of our proposed method are evaluated for predicting multiple component degradations when the
86 engine operates under variable operating and dynamical performance conditions for a period of up to 25,000

87 h. A series of prognosis performance metrics, as suggested by Saxena et al. [28], have also been developed
88 and implemented to assess the accuracy of the proposed prognosis scheme. The proposed prognostic method
89 has the capability to enhance and refine the current gas turbine performance prediction approaches, and to
90 improve and extend performance-based prognostic techniques.

91 To summarize, the main contributions of this paper are as follows. First, the prognosis of an engine
92 component performance degradation for an industrial gas turbine operating under dynamical conditions
93 is investigated by using an adaptive diagnostic and prognostic scheme. In contrast to our earlier works
94 [17, 18], where the concept of performance adaptation was developed and implemented only for diagnostics,
95 this study extends the corresponding scheme for prognostic purposes. Specifically we propose a sliding-
96 window based performance adaptation concept that can effectively deal with prediction of multiple engine
97 component degradations. Therefore, detecting and predicting the health of multiple engine components that
98 degrade with respect to time time under dynamical conditions through the use of a new sliding window based
99 performance adaptation method is developed and **examined for the first time in the literature, to the best of**
100 **the authors knowledge**. In contrast to other available prognostic approaches in the literature, such as those
101 in [9, 11, 12, 13, 14], our proposed scheme is capable of predicting effectively the component degradations
102 under dynamical operation and variable ambient conditions. By using a regression method for fitting the
103 diagnostic results of each diagnostic window, the health of each engine component can be accurately and
104 efficiently predicted. Finally, we assess the accuracy of our proposed prognosis scheme by evaluating the
105 equivalent RUL of each component and the probability of the distributed prognostic results to lie within the
106 acceptable levels of accuracy.

107 The remainder of this paper is organized as follows. In Section 2, the assumptions and the methodology
108 for the proposed scheme that integrates performance adaptation, diagnostic and prognostic capabilities is
109 described. The description of the case studies is presented in Section 3. Simulation results of the proposed
110 approach are presented in Section 4, followed by the conclusions in Section 5.

111 **2. Methodology**

112 *2.1. Assumptions*

113 Generally speaking, the gas turbine degradation is heavily influenced by various factors such as ambient
114 and operating conditions, manufacturing tolerances and imperfections that make the task of prognosis quite
115 challenging one. In this context, several prognostic schemes have been developed and applied for gas turbines
116 and this emphasizes the fact that there does not exist a unique approach to cover effectively such a wide
117 range of degradation scenarios. However, in order to make the proposed scheme more generic and applicable
118 to real engine applications the following assumptions are made in this study:

- 119 • Only soft engine performance degradations due to the compressor fouling and turbine erosion that are
120 developed over time are examined.
- 121 • The ambient conditions and engine operational mode are variable and dynamic, respectively and
122 represent the ever growing demand for flexibility in a gas turbine operation.
- 123 • The degradation patterns examined for the compressor fouling and turbine erosion are monotonically
124 increasing or decreasing depending on the examined type of component degradation.
- 125 • The degradation patterns that are examined are independent of maintenance actions and are mainly
126 attributed to the aging of the component. For instance, when the compressor is experiencing fouling
127 the lost efficiency and mass flow capacity cannot be fully recovered by offline washing and such an
128 unrecoverable degradation accumulates over time.
- 129 • The component degradations are described by deviations of isentropic efficiency and mass flow capacity
130 from their clean/healthy values.

131 2.2. Performance Adaptation

132 The concept of performance adaptation is the process of tuning the nonmeasurable component param-
133 eters, such as the mass flow capacity and isentropic efficiency, of an engine model in order to match the
134 measurable engine performance parameters, such as the temperature and pressure along the gas path, of a
135 reference engine. The process involves, invokes and implements an optimization algorithm for minimizing
136 the residuals between the performance parameters of the model and the reference engine, as depicted in Fig.
137 3. Such a method forms the foundation of refining an engine model and matching it to the engine under
138 investigation.

139 The advanced performance adaptation approach that is empowered by a novel component map generation
140 scheme is the one that was developed by the authors in [17, 18] and has been also used in this study. A
141 brief description of this method follows. Generally the engine behavior, assuming there is no presence of
142 measurement noise and bias, can be expressed as follows:

$$143 \mathbf{Y} = f(\mathbf{X}, \mathbf{u}) \tag{1}$$

144 where \mathbf{Y} denotes the engine performance vector consisting of the measurable parameters, \mathbf{X} denotes the
145 component characteristic vector that consists of nonmeasurable parameters and \mathbf{u} denotes the ambient and
146 operating conditions vector consisting of ambient conditions and a control input parameter called handle
147 that can be either fuel flow rate, rotational speed or any other quantity.

148 The engine performance vector can be either the field data of a service engine or simulations from a
different engine model. To conduct testing of our proposed method two engine models are used. The

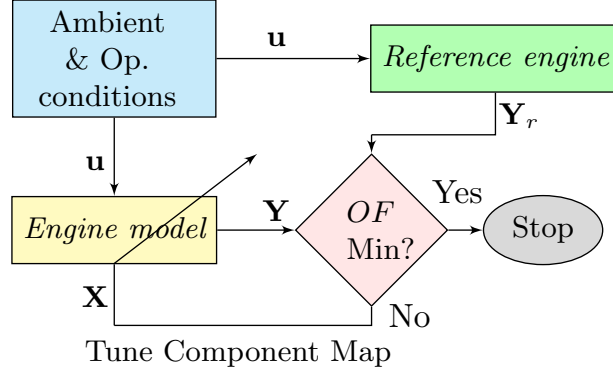


Figure 3: The flow chart of the performance adaptation process.

149 engine model that uses the performance maps of PROOSIS [29] gas turbine simulation software is going to
 150 be referred to as the *reference engine*. The second engine model implements the advanced map modeling
 151 method that was developed by the authors in [18] and is going to be referred to as the *engine model*.

For this study, the difference between the predicted \mathbf{Y} by the *engine model* and the observed \mathbf{Y}_r measurements from the *reference engine* is evaluated by means of an Objective Function (OF) that is defined as follows:

$$OF = \sqrt{\sum_{i=1}^n \left(\frac{\mathbf{Y}_i - \mathbf{Y}_{r_i}}{\mathbf{Y}_{r_i}} \right)^2} \quad (2)$$

152 where n denotes the total number of operating points and \mathbf{Y}_i and \mathbf{Y}_{r_i} denote the i -th predicted and
 153 measurable performance vector, respectively. Further details regarding the performance adaptation can be
 154 found in [17, 18].

155 2.3. Adaptive Diagnostics

156 Performance degradation of an engine component is represented by deviation of its parameters from their
 157 nominal/clean/healthy values. The deviation of a component parameter such as the mass flow capacity $\Delta\Gamma$
 158 can be expressed as the **absolute** difference between the degraded Γ_{deg} and the clean Γ_{cl} divided by the clean
 159 Γ_{cl} as follows, i.e. $\Delta\Gamma = |\Gamma_{deg} - \Gamma_{cl}| / \Gamma_{cl}$.

160 In order to emulate such a component degradation deviations in the mass flow capacity and efficiency
 161 of each component of the reference engine are injected. Therefore, the nominal/clean/healthy vector $\mathbf{X}_{r_{cl}}$
 162 which is the output of the component map is multiplied by a time dependent injected deviation signal
 163 $\Delta\mathbf{X}_{r_{inj}}$ that results in a deviated component vector $\mathbf{X}_{r_{deg}}$. Consequently, the *reference engine* operates at
 164 degraded conditions and produces a new set of degraded measurable parameters $\mathbf{Y}_{r_{deg}}$, as schematically
 165 depicted in Fig. 4.

166 The injected deviations of the component vector $\Delta\mathbf{X}_{r_{inj}}$ can be expressed as a function of time t , i.e.
 167 $\Delta\mathbf{X}_{r_{inj}} = g(t)$. The type of the function g depends on the degradation pattern that each component

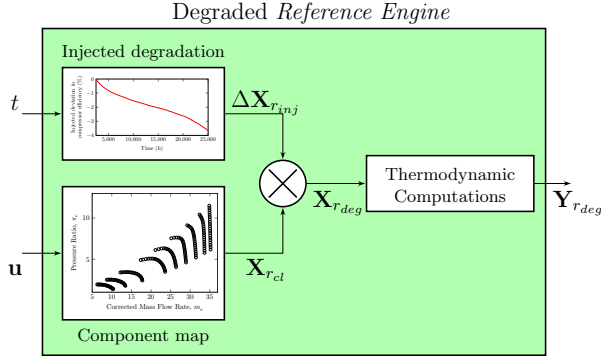


Figure 4: Representation of time dependent injected degradations into the engine component.

168 experiences. In this study component degradation patterns such as the ones shown in Fig. 5 will be
 169 examined. When the engine operates under dynamical conditions the degradation of the engine components
 170 evolves faster than that at steady state conditions, as shown in Fig. 5, where it is assumed that the rate
 171 of component degradation due to aging is represented as a drop of -1% per year in the health component
 172 parameter. The health component parameter simply refers to the mass flow capacity and the efficiency.
 173 Typical values of degradation rates with respect to the above health indicators depend on the engine type
 174 and its operating conditions [30]. The former observation highlights the importance and the challenging
 175 aspect of predicting the performance of engine degraded components when the gas turbine is operating at
 176 dynamical transient conditions.

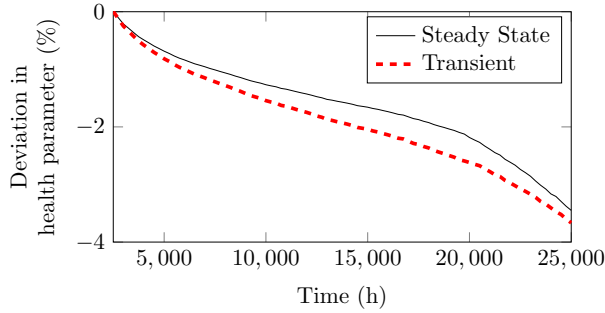


Figure 5: Typical engine health parameter deviation with respect to time for 25,000 h of steady state and transient engine operations.

177 The objective of the diagnosis problem is to determine the level of degradations that are injected in
 178 the components of the *reference engine*. This is achieved by minimizing the observed residuals between
 179 the component parameters of the *reference engine* and the *engine model* through implementation of the
 180 performance adaptation methodology [17].

181 It should be emphasized that the performance adaptation scheme has the capability of generating and
 182 tuning a set component maps to match the engine measurements for a wide range of operating conditions.

183 Once each component map is fed with its corrected rotational speed and pressure ratio inputs, its corre-
184 sponding outputs that are the mass flow rate and the efficiency are determined and subsequently used for
185 thermodynamic computations. For simulating the time evolving component degradation the outputs of the
186 maps are injected with time dependent signals as shown in Fig. 4, before their utilization for the thermo-
187 dynamic computations. Therefore, the degraded *reference engine* might operate under the same operating
188 conditions (inputs) as the clean *reference engine* but their outputs will be different since the time dependent
189 injected faults alter the initial clean/healthy output of the component map. The complexity of decomposing
190 the time parameter in the estimated degraded component parameters can be resolved by partitioning the
191 diagnostic results into smaller time increments so that the adaptation approach can handle. Therefore, in
192 this work a sliding window-based method is proposed that has the advantage of filtering out the effects that
193 time-dependent injected degradations have on the adaptation procedure.

194 From the bank of available degraded data, the diagnostics **tasks** are performed through a set consisting
195 of q sliding windows that cover the entire range of the available data. On a local level, each window that
196 is initiated at the time instant t_d has a width of L that includes n operating points as shown in Fig. 6.
197 The n operating points corresponding to each window refer to the samples of data that one may utilize
198 to perform the diagnostic analysis and is different from the total number of measurement data that are
199 available within the time frame of width L . The n operating points corresponding to each window refer to
200 the samples of data that one may utilize to perform the diagnostic analysis and is different from the total
201 number of measurement data that are available within the time frame of width L . The number of operating
202 points n selected for an analysis depends on how sensitive it would be to the data resolution. If the total
203 data captured in a time width L is of high resolution having repeated values and at the same time present
204 a uniform distribution, then one may reduce the data samples that are utilized for a diagnostic analysis
205 to a number n to reduce the computational time without sacrificing the diagnostic accuracy. Several data
206 reduction and smoothing techniques could be implemented for accomplishing the above. The above method
207 is more practical and suited for real applications given that the gas turbine users may not have access to
208 high quality engine data for covering a wide range of operational history of the engine.

209 For each diagnostic sliding window, the *engine model* matches the degraded measurements of the *refer-*
210 *ence engine* by generating a new set of component maps that form the degraded vector \mathbf{X}_{deg} . The initial
211 adaptation of the *engine model* is in fact a training phase for the fault diagnosis task given that it acts as
212 the reference frame for the engine healthy/clean condition.

213 Another key aspect of the above process is that the time t_d when the adaptive diagnosis is initiated and
214 the time t_e when the proposed scheme starts detecting the component degradation effectively are different.
215 This occurs due to the fact that the proposed diagnostic algorithm requires time to tune itself with the
216 degradation progression data before it can reach an accurate diagnosis. Therefore, the sliding windows for
217 diagnostic analysis overlap with one another at a data length of l as shown in Fig. 7. It follows that at

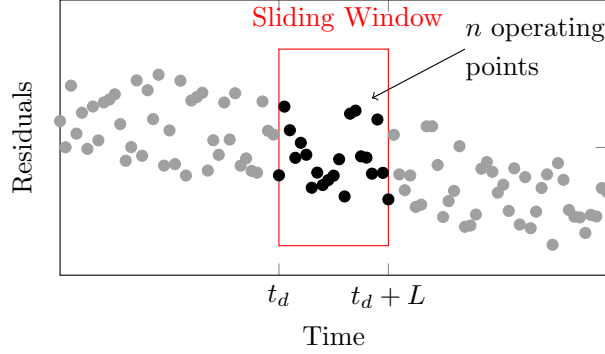


Figure 6: Representation of the sliding window-based diagnostic parameters.

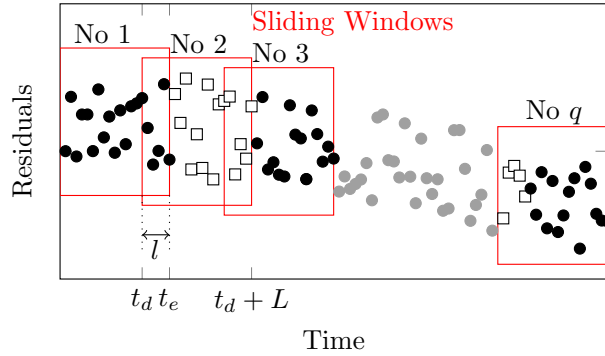


Figure 7: Representation of the overlap between the sliding windows that are used for the diagnostic problem.

218 the diagnostic window No. 2, the process is initiated at t_d and only the diagnostic information after t_e that
 219 is depicted as squares is considered. For the region between t_d and t_e , the diagnostic information refers to
 220 the previous window No. 1. This process is repeated until the final set of data is used in the final window
 221 No. q . A Diagnostic Index (DI) as described in [18] is now utilized to assess the accuracy of the diagnosis
 222 information and is defined as follows:

$$DI = 100 \left(\frac{1}{1 + \epsilon} \right) \quad (3)$$

223 where ϵ denotes the mean error in the component vector \mathbf{X} . **Consequently, the accuracy level that component**
 224 **maps are optimized to match the degraded measurements is evaluated according to:**

$$\epsilon = \frac{\sum_{i=1}^n \left| \frac{\Delta \mathbf{X}_{pred_i} - \Delta \mathbf{X}_{rinj_i}}{\Delta \mathbf{X}_{rinj_i}} \right|}{n} \quad (4)$$

225 2.4. Prognostics

226 Prognosis is concerned with the prediction of the engine future health that is analyzed with the adaptive
 227 performance diagnostic method for all the past operating points. The main objective of the adaptive

228 prognosis scheme is to forecast the performance of each engine component that degrades over time for a
 229 specific prognostic window.

230 Taking into consideration the fact that the sliding window-based diagnostic approach partitions the
 231 degradation pattern into smaller time increments, it is reasonable to assume that at such a local scale the
 232 engine components performance degrades linearly with time. In order to ensure that the degradation pattern
 233 will be linear at such a local scale, data analysis methods such as the Probability Density Functions (PDF),
 234 the skewness and kurtosis criteria [10] could be utilized to investigate the data distribution and estimate
 235 whether the rate of degradation satisfies the above assumption. Once this is performed then the data can
 236 be effectively handled by the sliding window diagnostic method. A wide spread PDF or sign changes in the
 237 skewness of data distribution [9] can indicate an increase or decrease in the degradation rate and can serve
 238 as guide for tuning the width L of the diagnostic windows. For this study, the diagnostic windows had fixed
 239 width L but one could easily modify this as stated above.

240 This observation allows one to perform the prognosis on a local window level instead of using the complete
 241 set of the past diagnostic windows. Therefore, a regression model can be used to determine the function h
 242 by which the degraded component parameter $\Delta\mathbf{X}_{lreg}$ varies with respect to time t as follows:

$$\Delta\mathbf{X}_{lreg} = h(t), t \in [t_d, t_d + L] \quad (5)$$

243 The linear regression method [9, 31] was implemented for this case. Therefore, the function h is obtained
 244 by:

$$h(t) = a_1t + a_2, t \in [t_d, t_d + L] \quad (6)$$

245 where the coefficients a_1 and a_2 are determined based on a least square minimization scheme. Once the
 246 degradation pattern is fitted accurately through the linear regression model, the health of the engine com-
 247 ponent is predicted for a prognostic window of time with width M . The accuracy of the prognosis is
 248 determined by comparing the obtained results with the actual *reference engine* degradation data $\Delta\mathbf{X}_{rinj}$
 249 and by determining the probability of this distribution to lie within specified accuracy bounds.

250 The next step of this process involves the utilization of the PDF in order to estimate the likelihood of the
 251 fitted regression model to take any given value. Among several probability distributions available, the most
 252 common for statistics and forecasting is the normal (Gaussian) distribution. The advantage of the normal
 253 distribution that has the characteristic bell-shape curve is that it is simple to manipulate mathematically and
 254 derive results that can be easily interpreted. Therefore, the normal distribution is going to be implemented
 255 in this study. The PDF of the normal distribution for a variable x is as follows:

$$f(x) = \left(\frac{1}{\sigma\sqrt{2\pi}} \right) e^{-\frac{1}{2} \left(\frac{x-\mu}{\sigma} \right)^2} \quad (7)$$

256 where x in this study refers to the degraded component parameter $\Delta\mathbf{X}_{lreg}$ and μ denotes its mean with a
 257 standard deviation of σ .

258 In order to compute the total probability of the distribution that lies within the specified **Accuracy**
 259 **Bounds (AB)** $[\alpha^-, \alpha^+]$ of the actual degradation, the PDF is integrated as follows:

$$p = \int_{\alpha^-}^{\alpha^+} f(x)dx \quad (8)$$

260 The integral has a maximum of 1 and a minimum of 0 when the entire PDF lies inside or outside the AB of
 261 the actual degradation, respectively. The actual degradation accuracy bounds at time t_p when prognosis is
 262 initiated are given by the following equations:

$$\alpha_{(t_p)}^- = x_{(t_p)}^\alpha - \alpha x_{(t_p)}^\alpha \quad (9)$$

263 and

$$\alpha_{(t_p)}^+ = x_{(t_p)}^\alpha + \alpha x_{(t_p)}^\alpha \quad (10)$$

264 where α denotes the level of accuracy and $x_{(t_p)}^\alpha$ refers to the actual deviation in the component parameter
 265 $\Delta\mathbf{X}_{r_{inj}}$ at the time instant t_p . The AB of 90% implies that the value of α is 0.10. It should be emphasized
 266 that in real gas turbine applications the component degradation $\Delta\mathbf{X}_{pred}$ can only be estimated and the
 267 actual degradation such as $\Delta\mathbf{X}_{r_{inj}}$ remains an unknown.

268 The AB of the actual degradation which is based on the injected degradation $\Delta\mathbf{X}_{r_{inj}}$ is not used here as
 269 a direct prognosis accuracy metric, but it is only an indication of how the prognostic results are distributed
 270 with respect to the actual degradation. Therefore, the PDF of the distributed prognostic results $\Delta\mathbf{X}_{lreg}$
 271 that are implemented here can serve as a guide for evaluating the width L of the diagnostic window that
 272 is used for the prognosis. A PDF that has a wide spread indicates that the past diagnostic window could
 273 be further partitioned into smaller time width L in order to achieve a PDF that has a narrower spread,
 274 and therefore the prognosis will be more reliable. A schematic representation of the PDF for the normal
 275 distribution of linearly regressed component parameter $\Delta\mathbf{X}_{lreg}$ with respect to the diagnostic predictions
 276 $\Delta\mathbf{X}_{pred}$ within the **AB** $[-\alpha, \alpha]$ corresponding to the actual degradation $\Delta\mathbf{X}_{r_{inj}}$ is shown in Fig. 8.

277 The final step in the prognostic process is to estimate the **RUL** of the engine components. Generally the
 278 gas turbine users have *a priori* information that is specified by the manufacturer for the **End of Life (EoL)**
 279 of the engine. This EoL criterion is associated with a performance threshold associated with the degraded
 280 component parameters $\Delta\mathbf{X}_{thr}$, beyond which maintenance actions should be performed. Majority of the
 281 gas turbine prognostic approaches [16, 32, 9] compute the RUL based on the estimate of the components
 282 degradation and by projecting the fitted degradation results to future. The latter is used in order to

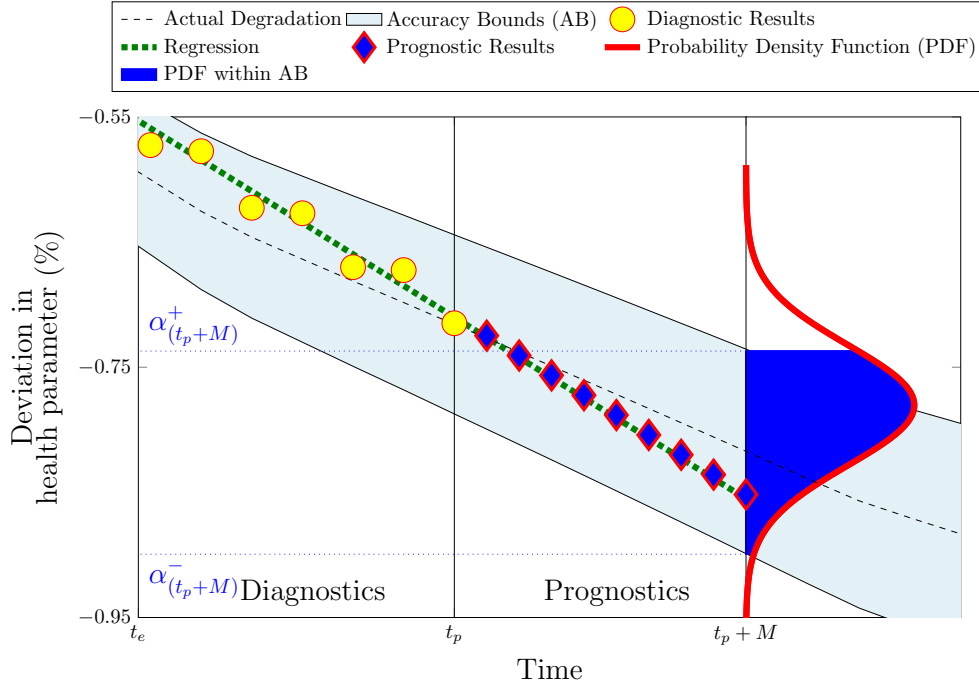


Figure 8: The PDF for the normal distribution of the degradation as predicted by the regression method at time t_p . The blue filled section of the curve represents the amount of this PDF that lies within the accuracy bounds $[\alpha^-, \alpha^+]$ of the actual degradation. The diagnostic results are depicted in yellow filled points.

283 evaluate how pessimistic or optimistic their prediction is with respect to the EoL which is normally based
 284 on steady state operation as presented by Li and Nilkitsaranont [9].

285 For a gas turbine operation that is dynamic the corresponding degradation pattern will change and
 286 consequently the RUL cannot be mapped to typical component degradation estimations that occur at
 287 steady state. Moreover, the main principle of our proposed prognostic scheme is to move away from conven-
 288 tional approaches [33] of projecting the fitted degradation pattern into future time until a specified value of
 289 the component degradation is reached and a probability is assigned to this final prediction. The proposed
 290 scheme is performed under a discrete window-based level that focuses on the pattern by which the engine
 291 components degrade over time and a PDF is assigned to the predicted degradation pattern itself at the end
 292 of each prognostic window.

293 Therefore, in this study we utilize an alternative methodology to the RUL metric that is designated as the
 294 Equivalent RUL (ERUL). This will be mapped only to the level of component degradation that is detected
 295 and not based on the projected line of the prognostic results that meets a specific level of degradation. Let
 296 us now make a reasonable assumption that if the diagnostic process is initiated at time t_d with a degraded
 297 health component parameter $x_{(t_d)}$, the threshold corresponding to the degraded health parameter $x_{(t_{EoL})}$
 298 would be reached at the maximum number of operating hours as suggested by the manufacturer EoL. This

299 is shown in Fig. 9.

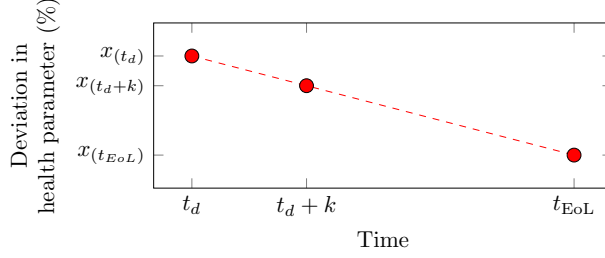


Figure 9: Representation of the component degradation parameters with respect to time as used for estimation of the ERUL.

300 The above assumption allows one to compute the ERUL at a time instant $t_d + k$ by associating it with
 301 the degradations that are detected as follows:

$$\text{ERUL}_{(t_d+k)} = -(t_{\text{EoL}} - t_d) \left(\frac{x(t_{\text{EoL}}) - x(t_d+k)}{x(t_{\text{EoL}}) - x(t_d)} \right) + (t_{\text{EoL}} - t_d) \quad (11)$$

302 where the variable $x(\cdot)$ refers to the degradations in the component parameters $\Delta \mathbf{X}_{lreg}$ as predicted by the
 303 regression method. **The major difference between the conventional RUL and our proposed ERUL is the fact
 304 that the latter is mapped directly to the degradation pattern at each time instant. Moreover, by taking into
 305 account that this pattern is partitioned into several linear segments one may compute the ERUL without
 306 having the entire operational history of the engine.**

307 Finally, accuracy bounds similar to the ones described earlier are utilized to represent the true ERUL
 308 that is based on the actual degradation of the component parameters $\Delta \mathbf{X}_{r_{inj}}$. Therefore, the ERUL for
 309 each component can be approximated by and compared with the true ERUL. The ERUL also reflects the
 310 rate that an engine component ‘consumes’ its life depending on the engine operating conditions.

311 To summarize, the prognosis procedure that is depicted in Fig. 10, is described as follows:

- 312 • Adapt the *engine model* to *reference engine* corresponding to a wide range of operating conditions.
 313 This will be used as the reference for future diagnostic analysis.
- 314 • The *engine model* is readapted to the new degraded conditions and match the component parameters
 315 of the degraded *reference engine* by implementing the sliding-window method.
- 316 • Once diagnosis is performed, the diagnostic results that are available in the diagnostic window are
 317 fitted by the regression method and the future health of each component is estimated. The prognostic
 318 window associated with the linear regression is determined by the user.
- 319 • The probability of the distributed prognostic results to lie within certain accuracy bounds of the actual
 320 degradation is assessed by implementing the PDF of the normal distribution.

- The capability of our proposed method to predict the engine health accurately is evaluated through the use of the RUL metric and the time before main maintenance actions can be estimated.

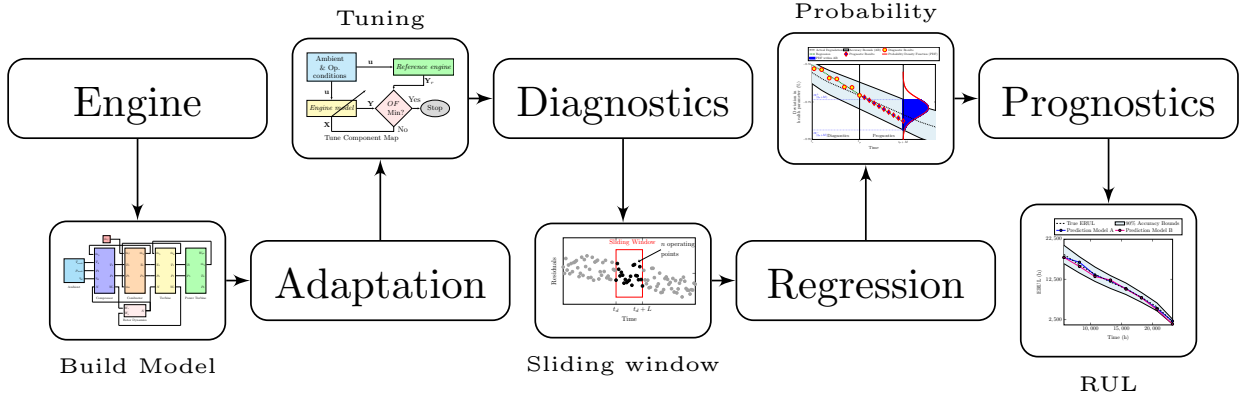


Figure 10: The flow chart of our proposed adaptive prognosis scheme.

2.5. Gas Turbine Model

The proposed diagnostic and prognostic approaches introduced and developed in previous subsections are now integrated with a dynamic model of a two shaft industrial gas turbine developed in Matlab/Simulink environment and validated with PROOSIS [29]. The average error that is observed between the PROOSIS measured output and the simulated output of the initial developed engine model was of the magnitude of 1% in [34] which was further reduced to 0.1% through the implementation of the performance adaptation in [26, 18]. The engine model consists of a compressor, a combustor, a compressor turbine and a power turbine as shown in Fig. 11. A detailed description of the model used for this application can be found in our earlier works in [34, 18].

3. Case Study Description

Our proposed prognosis scheme is implemented in a dynamic engine model [18, 34] and is evaluated and analyzed under transient conditions. Analysis of the diagnostic and prognostic results and discussions are provided in the subsequent results section 4.

One of the prerequisites for a successful adaptive diagnosis and prognosis scheme is that the engine measurable parameters are directly influenced by the component characteristic parameters to be adapted. Our primary objective for presenting the case studies is to evaluate and illustrate the achievable accuracy improvements of our proposed schemes that incorporate the performance adaptation, adaptive diagnostics and prognostics and take into consideration the above prerequisite. Therefore, the selection of the inlet and outlet measurements of the degraded components are well justified. The list of the selected input and

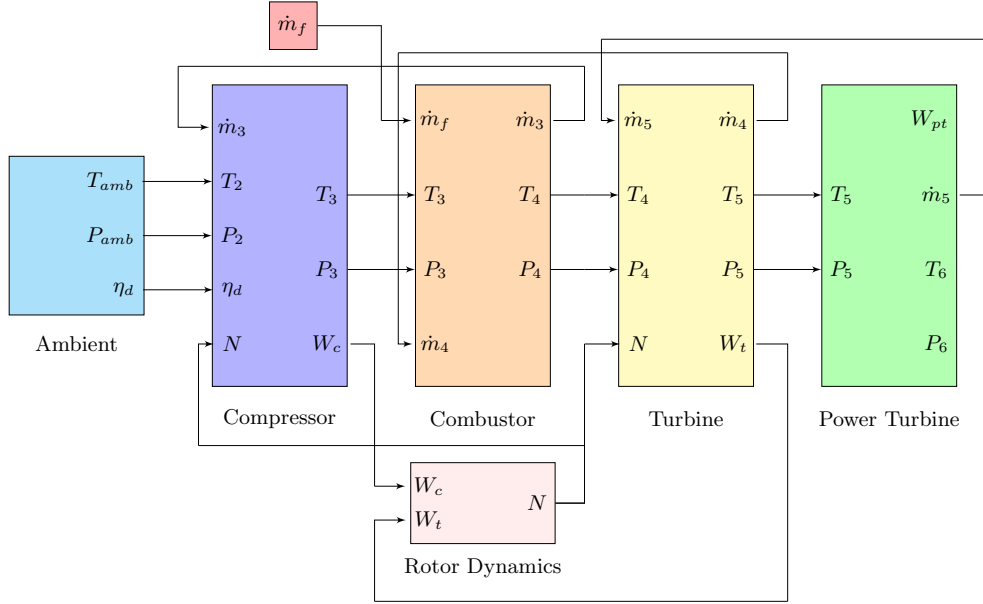


Figure 11: The two shaft industrial gas turbine engine model layout that is developed in Matlab/Simulink. For definitions of variables, refer to the Nomenclature section.

342 measurable parameters for the adaptive performance diagnosis and prognosis are provided in Tables 1 and
 343 2, respectively.

Table 1: The engine input parameters.

Symbol	Parameter	Units
P_{amb}	ambient pressure	Pa
T_{amb}	ambient temperature	K
\dot{m}_f	fuel flow	kg/s

344 Performance specifications of the *reference engine* are shown in Table 3. The nominal operating point
 345 that is chosen as the model design for this configuration is at 3.4 MW with the fuel flow rate \dot{m}_f set as
 346 the control input of the engine. At this point it should be noted that both diagnosis and prognosis are
 347 concerned with the difference Δ between the estimated and observed measured output of the engine and
 348 not the actual output itself. Consequently, the main objective of this scheme for assessing and evaluating
 349 the accuracy and performance of diagnosis and prognosis at dynamic operating conditions is independent of
 350 the actual measured parameters and design specifications of a gas turbine. The design specifications of a gas
 351 turbine play an important role in the model adaptation phase where component maps have to be generated
 352 and tuned to match the performance of such an engine. This is a topic that is extensively covered in our

Table 2: The engine performance measurable parameters.

Symbol	Parameter	Units
P_2	compressor inlet pressure	Pa
T_2	compressor inlet temperature	K
P_3	compressor discharge pressure	Pa
T_3	compressor discharge temperature	K
P_5	turbine exit pressure	Pa
T_5	turbine exit temperature	K
P_6	exhaust gas pressure	Pa
T_6	exhaust gas temperature	K
W_{pt}	power output	Watts
N	shaft rotational speed	rpm

Table 3: Performance specifications of the *reference engine*.

Symbol	Parameter	Value	Units
W_{pt}	Power	3.4	MW
π_c	Pressure Ratio	10.8	
η_{th}	Thermal efficiency	38	%
\dot{m}_4	Exh. flow rate	34	kg/s

earlier works. [18, 35].

It is important at this point to describe how the data corresponding to the *reference engine* are produced. The simulation step size that is used in Simulink for the case studies examined is set to 1 ms. The total simulation run time is 100 s and this results in 100,000 data samples. Since the objective of this study is to examine the maximum amount of degradation that each component is experiencing for a total of 25,000 h of operation, the available results should be correlated to represent this time interval. It is therefore assumed that 4 operating points correspond to one hour of operation. This implies that we capture the behavior of the engine every 15 minutes. The large size of the data samples ensures that the dynamic effects of the engine behavior are present during this analysis. For instance, a transient operating point at the time instant $t_1=1$ h will follow by another transient operating point at the time instant $t_2=1$ h and 15 min. On a global scale the collection of the operating points as the engine degrades over time are representative of the engine's dynamic behavior. This follows due to the fact that the selected fuel flow, which is the control parameter in

365 the simulation model, is random and highly nonlinear for this time interval. Therefore, the dynamic effects
 366 of the engine are not sacrificed during this correlation analysis and mapping of the available data.

367 It follows that in order, to make the case studies more realistic and representative of the dynamic engine
 368 behavior, both the ambient and operating conditions acting as inputs to the models are not considered
 369 constant and instead change with respect to time. The fuel flow schedule for this study is depicted in Fig.
 370 12. The ambient conditions are simulated so as to be periodic both on a daily basis as well as a yearly basis
 371 and the resulting ambient temperatures are shown in Fig. 13.

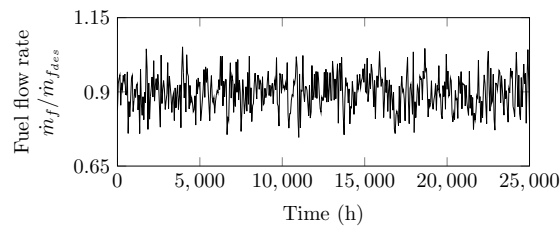
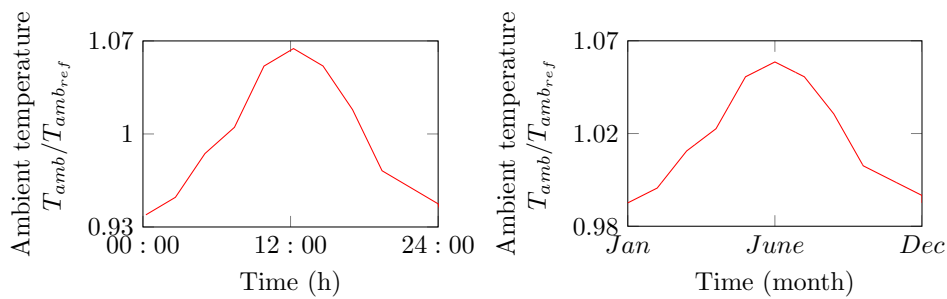
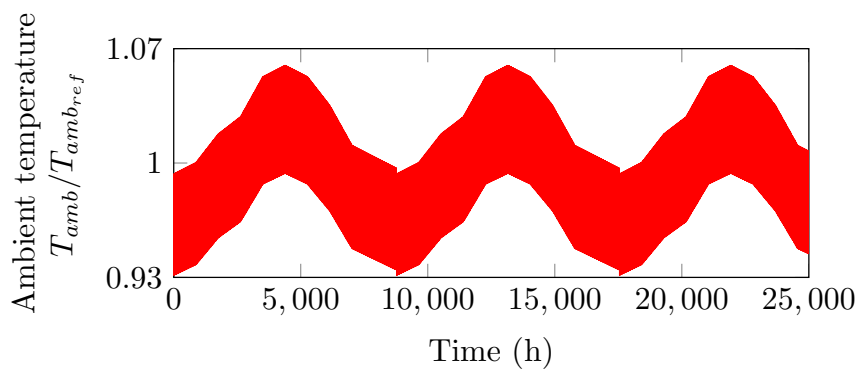


Figure 12: The variation of the fuel flow rate with respect to time.



(a) Temperature variation for 1 day.

(b) Temperature variation for 1 year.



(c) Temperature variations for 25,000 h.

Figure 13: The variation of ambient temperature with respect to time.

372 The required data for case studies are generated by performance simulations of the *reference engine* at

373 degraded conditions, where prognosis is performed at different instants of the data time series. The degraded
 374 conditions are represented by injecting deviations $\Delta\Gamma$ and $\Delta\eta$ in the mass flow capacity and efficiency into
 375 the *reference engine*, respectively. The range of injected deviations is summarized in Table 4.

Table 4: Injected deviations of the component parameters.

Component	Degradation	Parameter	Deviation Range (%)
Compressor	Fouling	$\Delta\Gamma_c$	0-(-1.8)
		$\Delta\eta_c$	0-(-2.7)
Turbine	Erosion	$\Delta\Gamma_t$	0-(2.5)
		$\Delta\eta_t$	0-(-1.8)
Power Turbine	Erosion	$\Delta\Gamma_{pt}$	0-(2.5)
		$\Delta\eta_{pt}$	0-(-2.7)

376 Two case studies are conducted. The objective of the first case study is evaluate the capability of the
 377 adaptive sliding window diagnostic method to detect accurately the injected degradations. The required
 378 measurements for the first case study are generated by performance simulations of the *reference engine* at
 379 degraded conditions.

380 The objective of the second case study is to prognose the performance behavior of each component
 381 based on the diagnostic results of the first case study. This is accomplished by the linear regression model
 382 on a local and discrete window-based method that takes into consideration only data from the previous
 383 diagnostic window. This specific proposed prognosis method will be designated as the Model A. In addition,
 384 the prognostic method that was suggested in [9], and that takes into account all the past diagnostic results
 385 on a global scale, is adopted and will be designated as the Model B, for facilitating its comparison with
 386 Model A.

387 In terms of the diagnostics, the Model B employs the adaptive diagnostic method that was developed by
 388 the authors and not the GPA method [9]. The GPA method that is used in [9] implements steady state data,
 389 however our adaptive diagnostic method can deal effectively with transient operations. This is conducted
 390 intentionally since uncertainty or improved accuracy that is provided by different diagnosis schemes should
 391 be filtered out in order to focus solely on the capability of each method to predict the engine performance,
 392 and therefore ensure that the comparisons among them are more realistic. The accuracy of the prognosis
 393 scheme is evaluated by means of the PDF and the RUL in order to compare these results with the actual
 394 degradation and actual RUL.

395 **4. Results and Discussion**

396 Our proposed prognosis scheme now is tested under dynamic transient conditions. The results for each
 397 case study are presented and discussed in the following subsections.

398 *4.1. Diagnostics - Case Study 1*

399 The objective of the first case study is to evaluate the accuracy of our proposed adaptive diagnostic
 400 methodology. This forms the foundation by which the prognosis will be developed and evaluated. Before
 401 commencing the diagnostic process, one needs first to adapt the *engine model* to the healthy *reference engine*
 402 for a wide range of operating conditions. This initial adaptation is the benchmark by which deviations in
 403 the component parameters will be determined subsequently. Therefore, degradation is injected to the engine
 404 component at $t_d=2,500$ h. The first set of data up to t_d is used for the initial adaptation of the *engine model*
 405 and represents the nominal/clean/healthy condition of the engine.

406 The diagnosis process is initiated at t_d on a sliding window manner, where the width L of the diagnostic
 407 window that is used here is $L=3,000$ h, and the length of their overlap is $l=500$ h. The total number of q
 408 diagnostic windows that are used is 9 and the number of operating points n that are utilized for detecting
 409 the degradation in each diagnostic window is 100.

410 The diagnostic results of this case study for the compressor isentropic efficiency are shown in Fig. 14.
 411 The capability of our developed adaptive diagnostic method that implements the sliding window method is
 412 clearly shown to be able to deal effectively with time dependent degradation process.

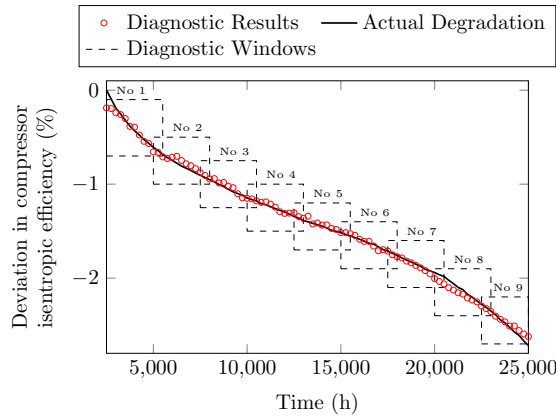


Figure 14: The compressor isentropic efficiency as predicted by our proposed diagnostic method for the specified windows.

413 The mean error for each diagnostic window is shown in Fig. 15, where it follows that the average error is
 414 below 0.1% for all diagnostic windows. As expected, the error is more evident in the first and the last group
 415 of diagnostic windows. The reason for this behavior is that for certain diagnostic windows the gradient of

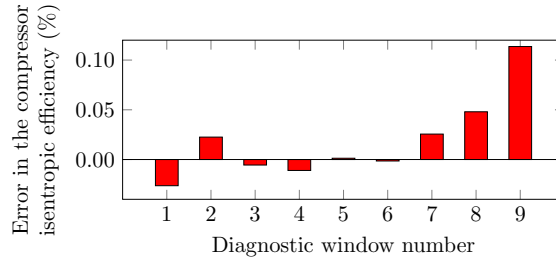


Figure 15: The average diagnostic error for the compressor isentropic efficiency for each diagnostic window.

416 the deviated component parameter is relatively greater than the other windows, and therefore this leads to
 417 a more challenging situation for the adaptive diagnostic method.

418 The diagnostic index associated with our proposed methodology for the compressor isentropic efficiency
 419 is obtained as 0.99. This implies that our diagnosis is 99% effective. The same level of diagnostic accuracy is
 420 achieved for all the degraded components of the engine. This case study results demonstrate the promising
 421 prospect of our adaptive diagnostic method for diagnosing accurately degradations of gas turbine engine
 422 components. This high accuracy performance of the diagnosis scheme is now shown to be transferable to
 423 the prognostics case study that follows in the next subsection.

424 4.2. Prognostics - Case Study 2

425 The objective of the second case study is to evaluate and demonstrate the accuracy of our proposed
 426 prognosis scheme under transient conditions. Prognosis is initiated at different data points instants based
 427 on the local or global past diagnostic results for Model A and Model B, respectively. The capability of our
 428 method is assessed by determining the accuracy of the prognosis subject to forecasting the performance of
 429 each component and then comparing it with the actual degradation as injected to the *reference engine*.

430 The prognosis process starts at $t_p=5,000$ h and is conducted every 2,500 h until one reaches the 22,500
 431 h of operation. Two prognostic windows of $M=1$ month and $M=2$ months width are used. In terms of the
 432 operation and maintenance strategy of industrial gas turbines the specific width M of the prognostic window
 433 corresponds to a practical time frame that facilitates gas turbine users to plan in advance for forthcoming
 434 maintenance activities depending on the engine condition.

435 The number of diagnostic results in each window that is utilized for forecasting the engine component
 436 performance is denoted by n and is set to 100. This number is always fixed for the Model A that implements
 437 only the diagnostic results of the previous diagnostic window. In case of Model B that builds upon the
 438 entire set of past data, the number n increases with respect to time. The compressor isentropic efficiency
 439 deviations that are predicted by Models A and B are shown in Figs. 16 and 17, corresponding to different
 440 initiations times.

441 As can be observed from Figs. 16 and 17, the Model A provides more accurate component performance

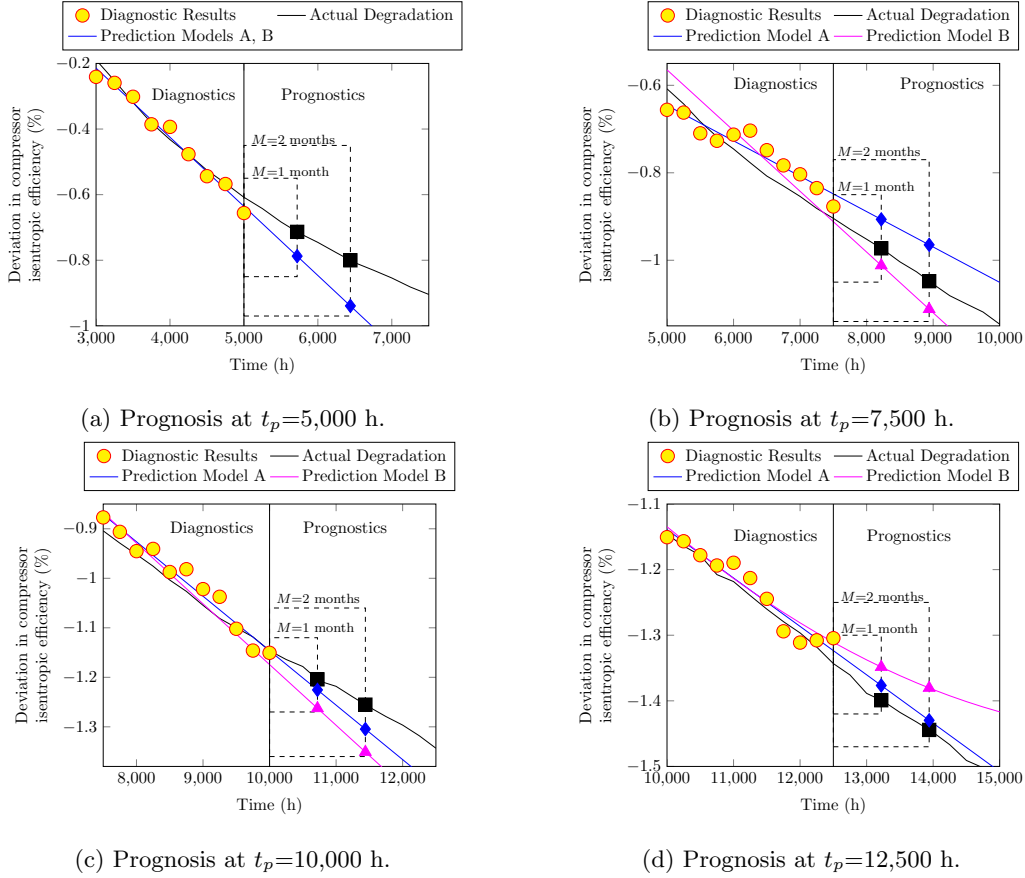


Figure 16: The predicted compressor isentropic efficiency for prognostic windows of width M when the process is initiated at $t_p=5,000, 7,500, 10,000$ and $12,500$ h of operation.

442 parameter predictions than Model B. This is actually expected since partitioning the degradation pattern
 443 into small increments of time ensures that the diagnostic results present a linear trend that can be cap-
 444 tured expeditiously and more accurately as compared to having the entire performance data of the engine
 445 component.

446 In contrast to the linear regression method of Model A, the regression fit of Model B ranges from linear
 447 corresponding to the first diagnostic window up to quadratic corresponding to the last diagnostic window.
 448 The mean errors in predicting the compressor isentropic efficiency for one month and two months prognostic
 449 windows, when both Models A and B are implemented, are shown in Figs. 18 and 19, respectively. It is
 450 clearly evident that Model A is more accurate as compared to Model B.

451 At this point it should be emphasized that both prognosis models are using the regression approach
 452 that fits the trends in the diagnostic results. Both Model A and B benefit significantly from the improved
 453 accuracy of the adaptive diagnostic method that was encapsulated in Figs. 14 and 15. However, if the
 454 diagnosis scheme is not this accurate then Model B will be influenced significantly more than Model A as

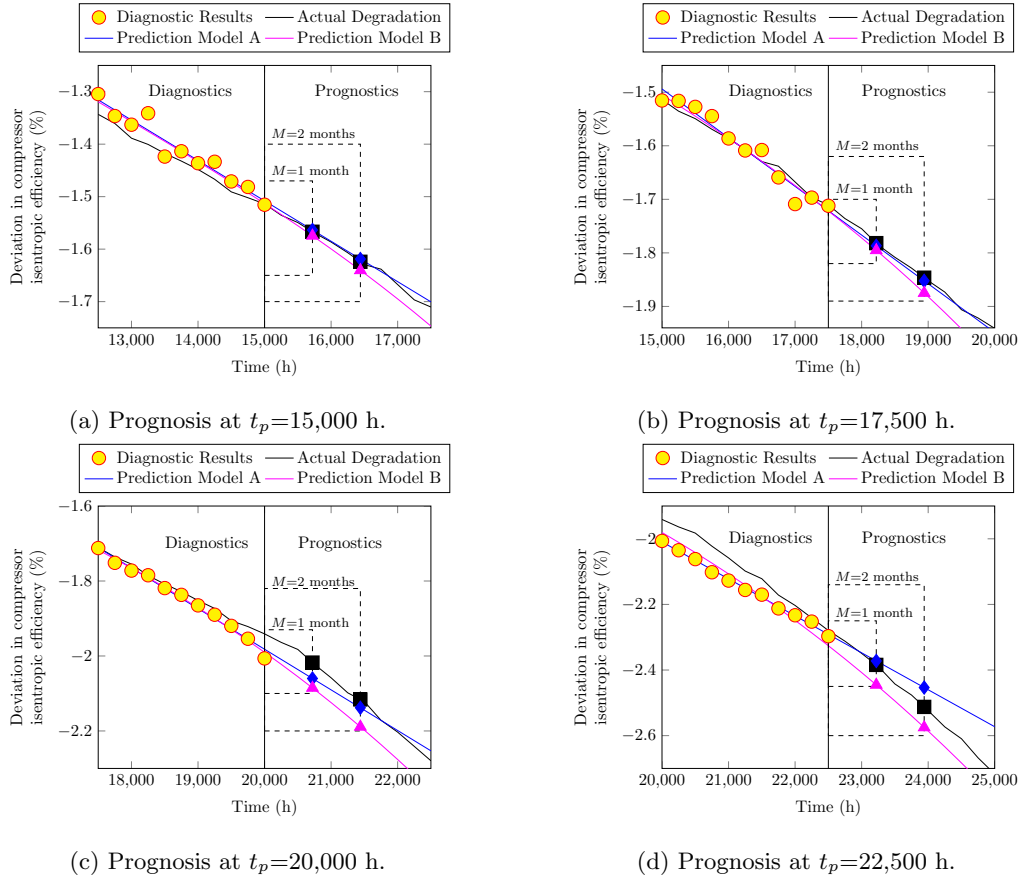


Figure 17: The predicted compressor isentropic efficiency for prognostic windows of width M when the process is initiated at $t_p=15,000, 17,500, 20,000$ and $22,500$ h of operation.

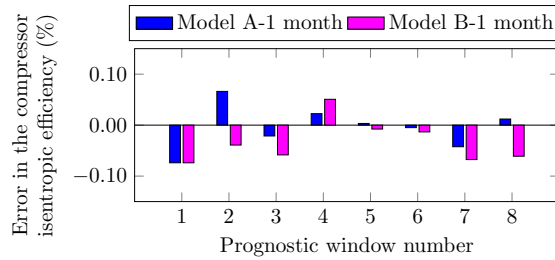


Figure 18: The prediction error for the compressor isentropic efficiency for $M=1$ month prognostic window.

455 it relies on a larger set of diagnostic data. In such a case, the error in the diagnosis scheme will accumulate
 456 significantly for all past diagnostic points where the prognosis of Model B is based upon.

457 It is therefore important to evaluate the probability of the prognostic results that lie within certain
 458 accuracy bounds corresponding to the actual degradation. For this case study where the accuracy bounds
 459 have been set at 90% of the actual degradation, the PDF for all the predicted component parameters lie

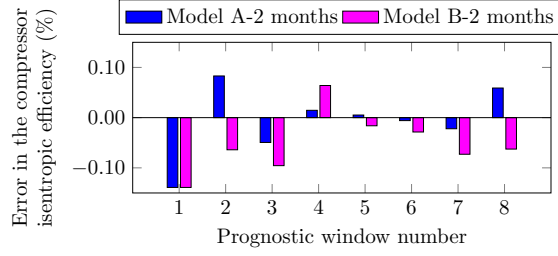


Figure 19: The prediction error for the compressor isentropic efficiency for $M=2$ months prognostic window.

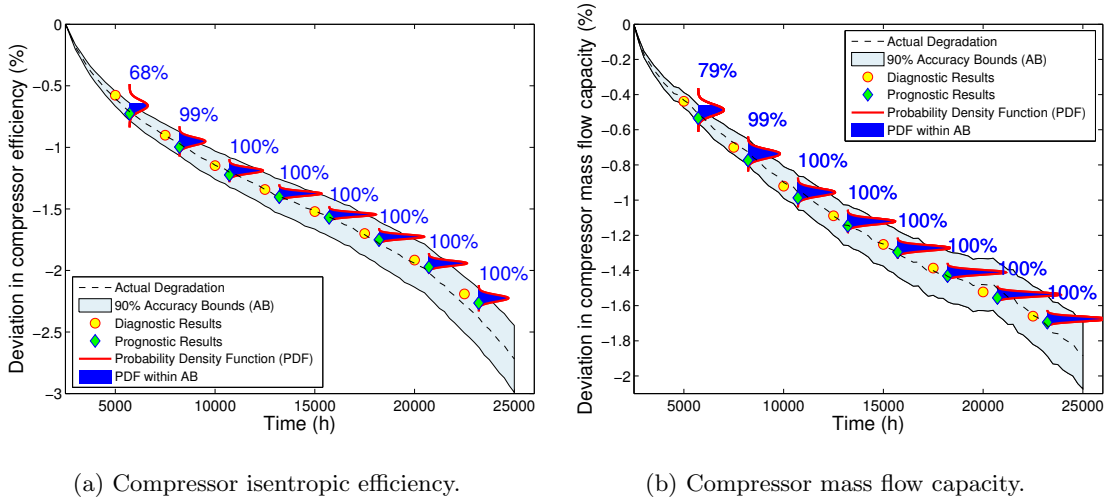
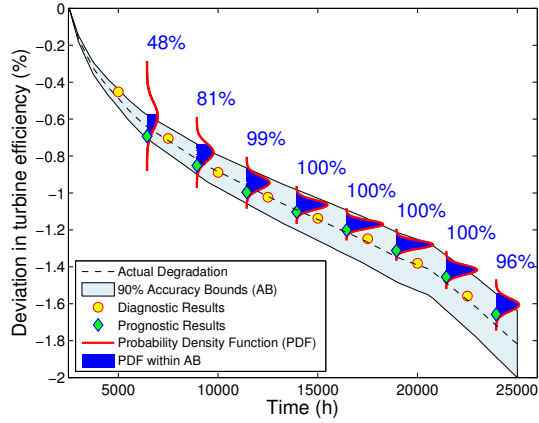


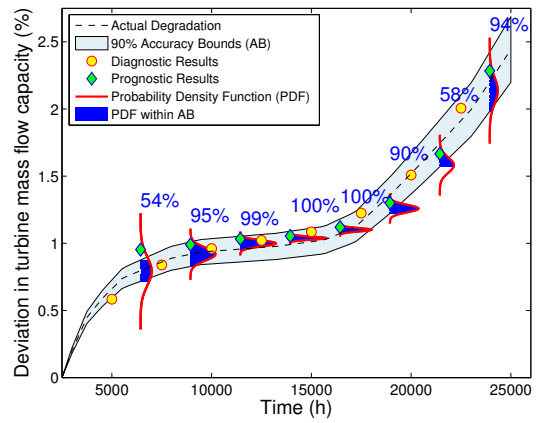
Figure 20: Probability distribution of the predicted compressor degradation with respect to the actual degradation for prognostic windows of width $M=1$ month. The red line represents the PDF of the predicted component parameter and the blue filled vertical slice represents its probability to lie within the accuracy bounds. The depicted diagnostic results correspond to the last detected degradation of the diagnostic window at $t_d + L$. Similarly, the prognostic results correspond to the last prediction of the prognostic window at $t_p + M$.

460 within these bounds as observed in Figs. 20, 21 and 22. As shown in Fig. 20, with the prognostic window of
 461 width $M=1$ month the probability starts from a moderate value at the first prognostic window and starts
 462 to reach 100% from the second prognostic window until the last set of data that are used for prognosis.
 463 Apart from the first prognostic window, the spread of the PDF for the compressor efficiency and mass flow
 464 capacity is quite small for a time frame of one month and representative of a reliable prognosis.

465 In case of the turbine and power turbine degradation where a 2 months prognostic window is depicted
 466 in Figs. 21 and 22, respectively, it is evident that initially the prognosis results lying within the accuracy
 467 bounds are moderate and they keep increasing with time. A closer look at the turbine and power turbine
 468 component degradations reveals the effects that specific diagnostic patterns have on the accuracy of the
 469 prognosis. For instance, there are regions along the path of each diagnostic pattern where the gradient of
 470 the deviated component parameter is significantly higher than the other regions. This implies that the rate

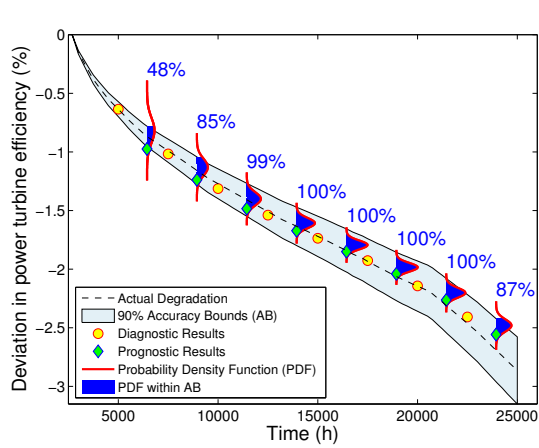


(a) Turbine isentropic efficiency.

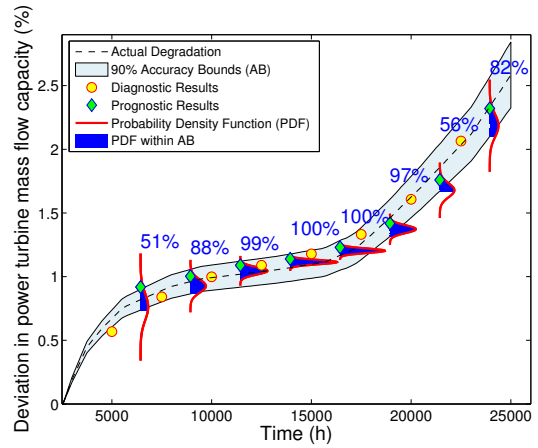


(b) Turbine mass flow capacity.

Figure 21: Probability distribution of the predicted turbine degradation with respect to the actual degradation for prognostic windows of width $M=2$ months. The red line represents the PDF of the predicted component parameter and the blue filled vertical slice represents its probability to lie within the accuracy bounds. The depicted diagnostic results correspond to the last detected degradation of the diagnostic window at $t_d + L$. Similarly, the prognostic results correspond to the last prediction of the prognostic window at $t_p + M$.



(a) Power turbine isentropic efficiency.



(b) Power turbine mass flow capacity.

Figure 22: Probability distribution of the predicted power turbine degradation with respect to the actual degradation for prognostic windows of width $M=2$ months. The red line represents the PDF of the predicted component parameter and the blue filled vertical slice represents its probability to lie within the accuracy bounds. The depicted diagnostic results correspond to the last detected degradation of the diagnostic window at $t_d + L$. Similarly, the prognostic results correspond to the last prediction of the prognostic window at $t_p + M$.

471 of degradation in these regions progresses faster than others. The latter affects the accuracy of the prognosis
 472 scheme given that it yields a wider spread of the PDF and the probability to lie within the accuracy bounds

473 is smaller.

474 One way to address this issue would be to add an additional criterion that will partition the diagnostic
475 pattern into even smaller time increments for regions in which the degradation propagates faster. Therefore,
476 the spread of the PDF can serve as a guide for modifying the width L of the diagnostic windows based on
477 the optimal level of gradient that is acceptable for achieving accurate diagnosis and prognosis results. An
478 additional metric that evaluates the accuracy of prognosis is the ERUL of the component. In case of the
479 compressor mass flow capacity the ERUL that is predicted by both Model A and Model B is shown in Fig.
480 23 for a one month prognostic window.

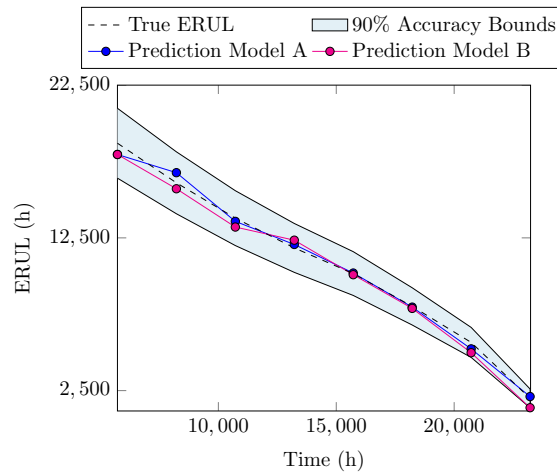


Figure 23: The ERUL of the compressor based on the compressor mass flow capacity as predicted by Model A and Model B for a 1 month prognostic window.

481 It follows from Fig. 23 that the Model A results lie within the true ERUL, whereas Model B is very
482 close to the true ERUL although it deviates slightly at the end of the prediction. The former observation is
483 further highlighted when one considers the relative error in the ERUL estimation as shown in Fig. 24. As the
484 prognosis process is initiated at different times instances t_p the relative error drops significantly for Model
485 A and lies within the 90% accuracy bounds. However, the ERUL prediction error for Model B, although
486 initially converges within the acceptable limits, does at later stages of the time series becomes significantly
487 higher than that of Model A.

488 Since the prognosis integrates a series of processes, the observed error is accumulated from the processes
489 of component map generation, engine model adaptation, and the diagnosis. This prediction error can be
490 traced back to the reconstruction and tuning of the model's component maps, and more specifically that
491 of the compressor which is more complex. Once the output of the compressor map is injected with time
492 evolving faults, the adaptive diagnostic process attempts, through the sliding window method, to decompose
493 the time variable from the estimated output of the map. During the above process it is important to analyze

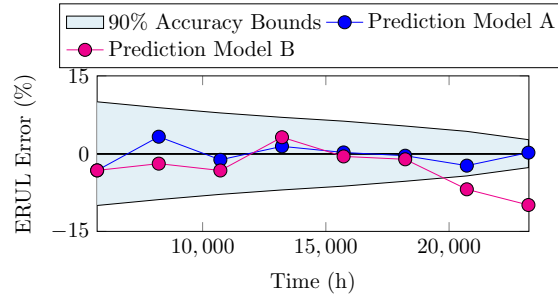


Figure 24: The relative error (%) in the ERUL of the compressor based on the compressor mass flow capacity as predicted by Model A and Model B for a 1 month prognostic window.

494 the pattern of the data available in each diagnostic window. If the available data correspond to accelerated
 495 or decelerated rate of degradation, this implies that the diagnostic pattern could be further partitioned into
 496 smaller time increments in order to facilitate the adaptive diagnostic process and reduce further the error.

497 It can be concluded that the performance of our proposed prognostic scheme is dependent upon the
 498 accuracy of the adaptive diagnostic method, that in turn relies heavily on the engine model. Therefore,
 499 it is crucial to continuously adapt the *initial engine model* to match the performance of the engine under
 500 investigation in order to establish a good benchmark for future diagnostic and prognostic analysis. Variable
 501 operating conditions make the adaptation of the *engine model* to the *reference engine* a challenging task.
 502 However, it gives a greater insight into the dynamics of the engine health and how this evolves with time.

503 As far as the practical aspects and limitations of our proposed scheme are concerned when used in real
 504 engines and real fault cases several considerations must be taken into account. Two key areas that need spe-
 505 cial attention for successfully implementing the proposed scheme are the data preprocessing and the engine
 506 model adaptation. Data preprocessing ensures that the data available from a service engine are properly
 507 corrected, smoothed, averaged and filtered out from noise and bias. One of the limitations of the proposed
 508 scheme is that it does not include a method for handling measurement noise and bias. This is something
 509 that can be successfully handled by Kalman filters, Neural Networks (NN), or other data-based methods at
 510 the preprocessing phase or in conjunction with the engine adaptation process and before the adaptive sliding
 511 window diagnostics. The width L of each diagnostic window can be adjusted based on the distribution of the
 512 available data for diagnosis so that the linear regression assumption made for prognosis will be adequately
 513 justified. A good quality set of engine data that is utilized by our proposed scheme is of crucial importance
 514 for the accuracy of diagnosis, and therefore for prognosis.

515 Another practical consideration deals with the maintenance activity of an engine from the time of the
 516 most recent model adaptation up to the time that the diagnosis and prognosis are pursued. For a unit that
 517 is on grid supporting operational modes with many transients this implies that the engine model should
 518 be adapted to the widest possible operational envelope. Another limitation of our proposed scheme is that

519 it is not readily applicable for detecting and predicting gas turbine performance that is below 50% of the
520 engine's rotational speed. This low operational speed regime is governed by a group of component maps
521 that are different than the ones implemented for the engine model adaptation and diagnosis. However, one
522 could utilize low speed component map generation methods for adapting and implementing the current
523 scheme to diagnose and prognose engine behavior at very low speeds. Finally, the engine model should be
524 continuously refined to its most recent health condition so that the prognosis could be performed with an
525 increased reliability and accuracy.

526 Therefore, implementation of our proposed scheme to any gas turbine performance simulation or as a
527 health monitoring, diagnosis and prognosis tool could provide a more reliable and accurate information for
528 gas turbine engines and supports the users in making more accurate decisions on efficiently managing their
529 assets.

530 **5. Conclusions**

531 In this paper, a novel prognostic scheme is introduced and developed that aims to improve the accuracy of
532 gas turbine engine performance prediction under dynamic operating conditions. The concept of an advanced
533 performance adaptation method is integrated with a dynamic gas turbine engine model that is developed
534 in Matlab/Simulink environment. An optimization methodology was utilized to match the dynamic engine
535 model to a reference model, that utilizes component characteristic maps that are available from the PROOSIS
536 and implemented as look up tables.

537 Testing of our proposed methods to a two shaft industrial gas turbine engine model operating for 25,000
538 h subject to multiple component degradations demonstrate the following observations. The component
539 degradation pattern is accurately captured by locally fitting linear regression functions at specific sliding
540 diagnostic windows. This is achieved by implementing a nonlinear unconstrained optimization method for
541 reconstructing the component map curves until the resulting simulated measurements match those of the
542 reference engine for each diagnostic window. The engine health is predicted accurately with a prognostic
543 window ranging from one month up to two months of operation.

544 The capability of our proposed schemes to adapt, diagnose and prognose the gas turbine performance
545 when this is represented by dynamic operating conditions gives a great insight into the dynamics of the
546 degradation pattern mechanisms. The implementation of our proposed method to any condition monitoring
547 and health estimation strategy could enhance the understanding of the gas turbine dynamic behavior, and
548 therefore could significantly improve the operational and maintenance strategy of gas turbine assets.

549 Acknowledgements

550 This publication was made possible by NPRP grant No. 4-195-2-065 from the Qatar National Research
551 Fund (a member of Qatar Foundation). The statements made herein are solely the responsibility of the
552 authors. The authors would also like to acknowledge the constructive comments, and suggestions provided
553 by the anonymous reviewers that greatly improved the quality of the article.

554 References

- 555 [1] A. Volponi, Gas turbine engine health management: Past, present, and future trends, *Journal of Engineering for Gas*
556 *Turbines and Power* 136 (5) (2014) 051201.
- 557 [2] Siemens, Flex Power Services for Siemens Fossil Power Plants, see also <http://www.energy.siemens.com/> (2013).
- 558 [3] GE, FlexEfficiency 60 A new standard of high efficiency and operational flexibility Portfolio, see also <http://www.ge.com/>
559 (2012).
- 560 [4] J. Simmons, K. Danai, In-flight isolation of degraded engine components by shape comparison of transient outputs, *Journal*
561 *of Engineering for Gas Turbines and Power* 134 (6) (2012) 061602.
- 562 [5] S. Borguet, M. Henriksson, T. McKelvey, O. Léonard, A study on engine health monitoring in the frequency domain,
563 *Journal of Engineering for Gas Turbines and Power* 133 (8) (2011) 081604.
- 564 [6] Y. G. Li, A gas turbine diagnostic approach with transient measurements, *Proceedings of the Institution of Mechanical*
565 *Engineers, Part A: Journal of Power and Energy* 217 (2) (2003) 169–177.
- 566 [7] G. Merrington, Fault diagnosis of gas turbine engines from transient data, *Journal of engineering for gas turbines and*
567 *power* 111 (2) (1989) 237–243.
- 568 [8] J. Janawitz, J. Masso, C. Childs, Heavy duty gas turbine operating and maintenance, Tech. rep., GE Power and Water
569 (2015).
- 570 [9] Y. G. Li, P. Nilkitsaranont, Gas turbine performance prognostic for condition-based maintenance, *J. Appl. Energy* 86 (10)
571 (2009) 2152–2161.
- 572 [10] A. Saxena, Prognostics the science of prediction, in: *Proc. PHM Conference*, Portland, OR, 2010.
- 573 [11] N. Daroogheh, N. Meskin, K. Khorasani, A novel particle filter parameter prediction scheme for failure prognosis, in:
574 *American Control Conference (ACC)*, 2014, IEEE, 2014, pp. 1735–1742.
- 575 [12] M. A. Zaidan, R. F. Harrison, A. R. Mills, P. J. Fleming, Bayesian hierarchical models for aerospace gas turbine engine
576 prognostics, *Expert Systems with Applications* 42 (1) (2015) 539 – 553.
- 577 [13] A. Vatani, K. Khorasani, N. Meskin, Health monitoring and degradation prognostics in gas turbine engines using dynamic
578 neural networks, in: *ASME Turbo Expo, GT2015-4401*, ASME, 2015.
- 579 [14] D. Zhou, H. Zhang, S. Weng, A novel prognostic model of performance degradation trend for power machinery maintenance,
580 *Energy* 78 (2014) 740–746.
- 581 [15] J. Dai, D. Das, M. Ohadi, M. Pecht, Reliability risk mitigation of free air cooling through prognostics and health man-
582 agement, *Applied Energy* 121 (2013) 104–112.
- 583 [16] C. Hu, G. Jain, P. Tamirisa, T. Gorka, Method for estimating capacity and predicting remaining useful life of lithium-ion
584 battery, *Applied Energy* 126 (2014) 182–189.
- 585 [17] E. Tsoutsanis, N. Meskin, M. Benammar, K. Khorasani, Transient gas turbine performance diagnostics through nonlinear
586 adaptation of compressor and turbine maps, *Journal of Engineering for Gas Turbines and Power*, GTP-14-1630 137 (9)
587 (2015) 091201.

- 588 [18] E. Tsoutsanis, N. Meskin, M. Benammar, K. Khorasani, A component map tuning method for performance prediction
589 and diagnostics of gas turbine compressors, *Applied Energy* 135 (2014) 572–585.
- 590 [19] L. Marinai, D. Probert, R. Singh, Prospects for aero gas-turbine diagnostics: a review, *Applied Energy* 79 (1) (2004) 109
591 – 126.
- 592 [20] Z. S. Vanini, N. Meskin, K. Khorasani, Multiple-model sensor and components fault diagnosis in gas turbine engines using
593 autoassociative neural networks, *Journal of Engineering for Gas Turbines and Power* 136 (9) (2014) 091603.
- 594 [21] S. Ogaji, L. Marinai, S. Sampath, R. Singh, S. Probert, Gas-turbine fault diagnostics: a fuzzy-logic approach, *Applied*
595 *Energy* 82 (1) (2005) 81 – 89.
- 596 [22] S. Ogaji, S. Sampath, R. Singh, D. Probert, Novel approach for improving power-plant availability using advanced engine
597 diagnostics, *Applied Energy* 72 (1) (2002) 389 – 407.
- 598 [23] G. Merrington, O. K. Kwon, G. Goodwin, B. Carlsson, Fault detection and diagnosis in gas turbines, *Journal of Engineering*
599 *for Gas Turbines and Power* 113 (2) (1991) 276–282.
- 600 [24] S. Sampath, Y. G. Li, S. Ogaji, R. Singh, Fault diagnosis of a two spool turbo-fan engine using transient data: A
601 genetic algorithm approach, in: *ASME Turbo Expo 2003, collocated with the 2003 International Joint Power Generation*
602 *Conference*, American Society of Mechanical Engineers, 2003, pp. 351–359.
- 603 [25] D. L. Simon, S. Borguet, O. Léonard, X. F. Zhang, Aircraft engine gas path diagnostic methods: Public benchmarking
604 results, *Journal of Engineering for Gas Turbines and Power* 136 (4) (2014) 041201.
- 605 [26] E. Tsoutsanis, N. Meskin, M. Benammar, K. Khorasani, An efficient component map generation method for prediction of
606 gas turbine performance, in: *ASME Turbo Expo 2014, GT2014-25753*, ASME, 2014, p. V006T06A006.
- 607 [27] J. Finn, F. Wagner, W. Basilly, Monitoring strategies for a combined cycle electric power generator, *Applied Energy* 87
608 (2010) 2621–2627.
- 609 [28] A. Saxena, J. Celaya, E. Balaban, K. Goebel, B. Saha, S. Saha, M. Schwabacher, Metrics for evaluating performance
610 of prognostic techniques, in: *Prognostics and health management, 2008. PHM 2008. International conference on*, IEEE,
611 2008, pp. 1–17.
- 612 [29] PROOSIS, Propulsion Object-Oriented Simulation Software, see also <http://www.proosis.com/> (2015).
- 613 [30] N. Aretakis, G. Doumouras, I. Roumeliotis, K. Mathioudakis, Compressor washing economic analysis and optimization
614 for power generation, *J. Appl. Energy* 95 (2012) 77–86.
- 615 [31] D. C. Montgomery, G. C. Runger, *Applied statistics and probability for engineers*, John Wiley & Sons, 2010.
- 616 [32] R. Joly, S. Ogaji, R. Singh, S. Probert, Gas-turbine diagnostics using artificial neural-networks for a high bypass ratio
617 military turbofan engine, *Applied Energy* 78 (4) (2004) 397 – 418.
- 618 [33] A. K. Jardine, D. Lin, D. Banjevic, A review on machinery diagnostics and prognostics implementing condition-based
619 maintenance, *Mechanical systems and signal processing* 20 (7) (2006) 1483–1510.
- 620 [34] E. Tsoutsanis, N. Meskin, M. Benammar, K. Khorasani, Dynamic performance simulation of an aeroderivative gas turbine
621 using the matlab simulink environment, in: *Proc. ASME IMECE, IMECE2013-64102*, Vol. 4, San Diego, USA, 2013, p.
622 V04AT04A050.
- 623 [35] E. Tsoutsanis, Y. G. Li, P. Piliadis, M. Newby, Part-load performance of gas turbines: part 2 multi-point adaptation with
624 compressor map generation and ga optimization, in: *Proc. ASME Gas Turbine India*, Vol. 1, Mumbai, India, 2012, pp.
625 743–751.